 MCB, vol.16, no.1, pp.13-26, 2019

Characterizing the Mechanical Variations of Human Femoropopliteal Artery During Aging Process

Shaoxiong Yang[1], Yingxin Qi[2], Zonglai Jiang[2] and Xiaobo Gong[1, *]

Abstract: Vascular diseases during aging process are closely correlated to the age-related changes of mechanical stimuli for resident cells. Characterizing the variations of mechanical environments in vessel walls with advancing age is crucial for a better understanding of vascular remodeling and pathological changes. In this study, the mechanical stress, strain, and wall stiffness of the femoropopliteal arteries (FPAs) were compared among four different age groups from adolescent to young, middle-aged, and aged subjects. The material parameters and geometries adopted in the FPA models were obtained from published experimental results. It is found that high mechanical stress appears at different layers in young and old FPA walls respectively. The characteristics of the middle-aged FPA wall suggests that it is the most capable of resisting high blood pressures and maintaining a mechanical homeostasis during the entire life span. It is demonstrated that the variations of stress and strain rather than that of wall stiffness can be used as an indicator to illustrate the profile of FPA aging. Our results could serve as an age-specific mechanical reference for vascular mechanobiological studies, and allow further exploration of cellular dysfunctions in vessel walls during aging process.

Keywords: Femoropopliteal artery, aging, mechanical stress and strain, wall stiffness, vascular mechanobiology.

1 Introduction

Aging is an irreversible biological process which correlates with the mechanobiological variation of cells and tissues through the changes of mechanical environments in different scales. Although numerous experiments *in vitro* have shown that mechanical stimuli play significant roles in vascular remodeling and disease development through cellular mechanotransduction [Sears and Kaunas (2016); Kumar, Placone and Engler (2017)], the variations in mechanical environments remain ambiguous during the aging process. Quantifying the effects of aging on the variations of the mechanical stimuli in the vessel wall is important for mechanobiological studies of age-related vascular disorders.

[1] Key Laboratory of Hydrodynamics (Ministry of Education), Department of Engineering Mechanics, School of Naval Architecture, Ocean and Civil Engineering, Shanghai Jiao Tong University, Shanghai, 200240, China.

[2] Institute of Mechanobiology and Biomedical Engineering, School of Life Sciences and Biotechnology, Shanghai Jiao Tong University, Shanghai, 200240, China.

[*] Corresponding Author: Xiaobo Gong. Email: x.gong@sjtu.edu.cn.

The cell-tissue interaction during vascular aging is too comprehensive and remains unclear, but the structural remodeling and the changes of mechanical properties with age have attracted considerable attention. Clinical studies suggested that stiffening of large arteries is one of the most prominent changes during aging, and vessel stiffness/elasticity serves as an independent index in evaluating the risk of cardiovascular diseases [McEnier, Yasmin, Qasem et al. (2005)]. Tarumi et al. [Tarumi, Ayaz Khan, Liu et al. (2014)] found that central arterial stiffening in senior groups enhances the pulsatility of cerebral blood flow and elevates the risk of brain damage. Wheeler et al. [Wheeler, Mukherjee, Stroud et al. (2015)] observed that aging increases thoracic aortic diameter and wall thickness while it decreases aortic contractility. These results indicate that the resident cells in vessel wall experience age-specific mechanical variations. Referring to the stress-growth law [Fung (2016)], the magnitude of mechanical stimuli nonlinearly correlates to the cell responses, and determines cell fate. In order to improve our understanding of the pathological changes associated with cellular mechanotransduction in vascular aging, it is important to characterize the mechanical environments of vascular cells over the population from young to old groups and compare their differences.

Recently the biomechanical characteristics of human femoropopliteal artery (FPA) aging have been widely studied due to the high failure rate of surgical interventions [Kamenskiy, Seas, Deegan et al. (2017); Desyatova, MacTaggart, Romarowski et al. (2018); Desyatova, MacTaggart and Kamenskiy (2017); Kamenskiy, Pipinos, Dzenis et al. (2015)]. Kamenskiy et al. [Kamenskiy, Seas, Deegan et al. (2017)] found that wall stiffness of FPAs in the circumferential direction is seldom affected by the age-related histological changes in elastin degradation and collagen addition. Their results could be explained as follows. Firstly, the FPAs, as peripheral muscular arteries, contain less amount of elastin than elastic arteries [Hayashi, Sugawara, Komine et al. (2005)]; and secondly, the collagen turnover with age seems to mainly contribute to the accumulation of the longitudinal collagen [Kamenskiy, Seas, Deegan et al. (2017)]. Therefore, wall stiffness alone may not be sufficient in characterizing the FPA aging. With biaxial mechanical testing, Kamenskiy et al. [Kamenskiy, Seas, Deegan et al. (2017)] provided detailed constitutive parameters for computational modeling of human FPA aging. The average circumferential stress across the wall thickness was found to present no significant correlation with age, and the stress and strain distributions in intima, media, and adventitia were not discussed in detail.

In this study, the effects of aging on the mechanical environments in the FPA wall are quantified to establish an age-specific mechanical reference for vascular mechanobiological studies. An aging index is further proposed for illustrating the FPA aging progress, and the ages corresponding to distinct mechanical properties are highlighted. In Section 2, the human FPAs aged from 11 years to 70 years old in the literature are adopted, and their *in vivo* stress responses are solved analytically based on nonlinear continuum mechanics. In Section 3, the variations in mechanical stress, strain, and wall stiffness during FPA aging are presented. In Section 4, the biomechanical characteristics of the FPA wall are discussed separately for different age groups, and the associated cellular mechanotransductions are revealed.

2 Methods

2.1 FPA geometries and constitutive relations

The relevant configurations of the arterial wall are illustrated in Fig. 1. Following [Kamenskiy, Seas, Deegan et al. (2017); Desyatova, MacTaggart, Romarowski et al. (2018)], the human FPA is modeled as a thick-walled straight tube with residual stress, which is reinforced by four families of fibers, including the axial ($\gamma_1 = 0$) and circumferential ($\gamma_2 = \pi/2$) fibers, and two families of fibers oriented helically ($\gamma_3 = -\gamma_4 = \gamma$), as illustrated in Fig. 1(b).

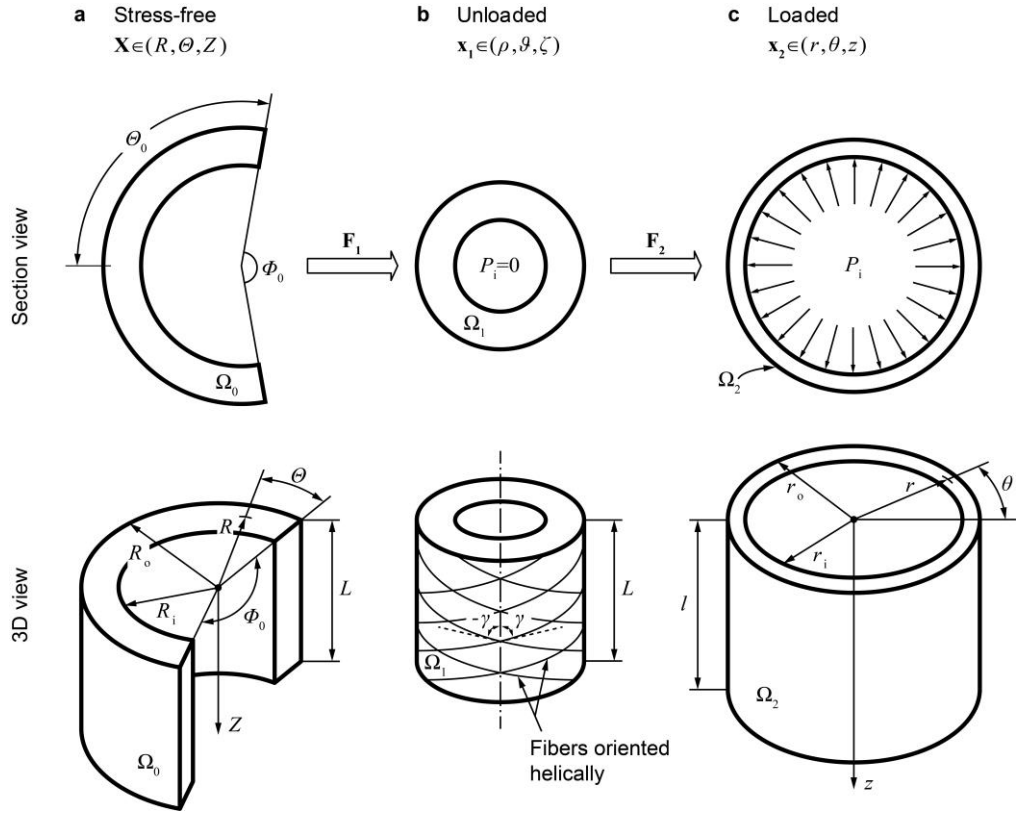

Figure 1: Arterial wall in (**a**) the stress-free configuration Ω_0 , (**b**) the unloaded configuration Ω_1 , and (**c**) the loaded configuration Ω_2 with internal blood pressure P_i . Φ_0 is the opening angle with $\Theta_0 = \pi - \Phi_0/2$; The stretch ratio $\lambda_z = l/L$ is used to quantify the axial extension; The fiber angle γ in the unloaded configuration is assumed to be the same as that in the stress-free configuration

Referring to the work of Kamenskiy et al. [Kamenskiy, Seas, Deegan et al. (2017)], the experimental data of human FPAs adopted in this study are from predominantly male donors. The measured FPA geometries are summarized in Tab. 1. They are used for

stress analysis during FPA aging from 11 years to 70 years, including adolescent (11~20 years), young (21~40 years), middle-aged (41~60 years), and elderly individuals (>60 years). It should be noted that the FPA radius in Tab. 1 exhibits an increase with age, which is consistent with other experimental results [Wheeler, Mukherjee, Stroud et al. (2015); Bortolotto, Hanon, Franconi et al. (1999)].

The constitutive formulation containing four exponential functions is used to describe the wall stiffening effect of human FPAs [Kamenskiy, Seas, Deegan et al. (2017)]:

$$\begin{aligned}\psi &= W\left(\mathbf{C},\mathbf{M}_i\right)-\frac{1}{2}p\left(I_3-1\right)\\ &= \frac{c_0}{2}\left(I_1-3\right)+\sum_{i=1}^{4}\frac{m_i c_{i1}}{4c_{i2}}\left\{\exp\left[c_{i2}\left(I_{i4}-1\right)^2\right]-1\right\}-\frac{1}{2}p\left(I_3-1\right)\end{aligned}. \tag{1}$$

Here, I_1 and I_3 are the first and third invariants of the right Cauchy-Green tensor $\mathbf{C}$, respectively; $I_{i4}\left(\mathbf{C},\mathbf{a}_i\right)=\mathbf{a}_i\cdot\mathbf{C}\mathbf{a}_i$ represents the square of the fiber stretch, and the unit vector $\mathbf{a}_i=\left[0 \quad \sin\gamma_i \quad \cos\gamma_i\right]^{\mathrm{T}}$ describes the *i*-th fiber direction; The tensor product $\mathbf{M}_i=\mathbf{a}_i\otimes\mathbf{a}_i$ characterizes the fiber structure; A Lagrange multiplier p is introduced to ensure the incompressibility constraint $I_3=1$; The material parameters c_0, c_{i1}, c_{i2}, and γ of human FPAs for different age groups are taken from the results of biaxial tests [Kamenskiy, Seas, Deegan et al. (2017)], as listed in Tab. 1. Assuming that the fibers arranged in helical structures exhibit the equivalent mechanical properties, we have $c_{41}=c_{31}$ and $c_{42}=c_{32}$. In addition, the exponential terms in Eq. (1) only contribute when the fibers are subjected to extension [Holzapfel, Gasser and Ogden (2000)], that is

$$m_i=\begin{cases}1 & \text{when } I_{i4}>1\\ 0 & \text{when } I_{i4}\le 1\end{cases}. \tag{2}$$

Table 1: Geometries and material parameters of human FPAs aged from 11 years to 70 years [Kamenskiy, Seas, Deegan et al. (2017)]

Age groups (Mean age), years	R_o, mm	R_i, mm	Φ_0, °	λ_z	c_0, kPa	c_{11}, kPa	c_{12}	c_{21}, kPa	c_{22}	c_{31}, kPa	c_{32}	γ, °
11-20 (16.7)	3.83	2.43	122.33	1.53	10.51	20.92	0.22	2.34	1.76	3.32	2.05	60.84
21-30 (25.0)	4.63	3.35	142.21	1.39	16.81	17.35	0.69	7.72	3.68	3.80	3.28	50.17
31-40 (35.7)	5.33	3.89	152.98	1.36	9.96	17.57	0.99	4.74	2.81	2.45	4.10	55.88
41-50 (47.2)	5.74	4.34	155.85	1.27	13.46	14.54	2.41	8.20	7.29	2.31	9.96	46.84
51-60 (56.1)	5.95	4.41	155.15	1.19	10.69	20.77	3.60	11.58	8.38	3.28	13.19	45.62
61-70 (64.6)	7.16	5.50	173.13	1.15	7.83	24.81	5.73	16.82	12.56	5.24	21.76	46.58

2.2 Deformation and stress response

An arterial segment excised from the human body generally reserves considerable residual stress [Chuong and Fung (1983)], and it can spring open and release most of the residual stress after a radial cut [Han and Fung (1996)], resulting in a nearly stress-free sector. Taking the opened-up sector in Fig. 1(a) as the reference configuration, the deformation gradient for the loaded arterial segment in Fig. 1(c) is

$$\mathbf{F}=\begin{bmatrix} \dfrac{\partial r}{\partial R} & \dfrac{1}{R}\dfrac{\partial r}{\partial \Theta} & \dfrac{\partial r}{\partial Z} \\ r\dfrac{\partial \theta}{\partial R} & \dfrac{r}{R}\dfrac{\partial \theta}{\partial \Theta} & r\dfrac{\partial \theta}{\partial Z} \\ \dfrac{\partial z}{\partial R} & \dfrac{1}{R}\dfrac{\partial z}{\partial \Theta} & \dfrac{\partial z}{\partial Z} \end{bmatrix}=\begin{bmatrix} \dfrac{\partial r}{\partial R} & 0 & 0 \\ 0 & \dfrac{\pi r}{\Theta_0 R} & 0 \\ 0 & 0 & \lambda_z \end{bmatrix}, \tag{3}$$

in which $r=r(R)$, $\theta=\dfrac{\pi}{\Theta_0}\Theta$, $z=\lambda_z Z$, and note that the plane strain assumption is adopted [Han and Fung (1996)].

Using the incompressibility constraint $\det\mathbf{F}\equiv 1$ in Eq. (3) yields

$$\partial r/\partial R=\Theta_0 R/\left(\pi r\lambda_z\right). \tag{4}$$

Integrating Eq. (4) with respect to R results in

$$r_{\mathrm{o}}^2-r_{\mathrm{i}}^2=\frac{\Theta_0}{\pi\lambda_z}\left(R_{\mathrm{o}}^2-R_{\mathrm{i}}^2\right). \tag{5}$$

It is desirable to introduce the second Piola-Kirchhoff stress tensor

$$\mathbf{S}=2\frac{\partial\psi}{\partial\mathbf{C}}=2\left(W_1\mathbf{I}+\sum_{i=1}^{4}W_{i4}\mathbf{M}_i\right)-p\mathbf{C}^{-1}, \tag{6}$$

where $W_1=\partial W/\partial I_1$, $W_{i4}=\partial W/\partial I_{i4}$, p denotes a Lagrange multiplier, and $\mathbf{I}$ denotes an identity matrix.

After a Piola transformation of Eq. (6), we obtain the Cauchy stress tensor $\boldsymbol{\sigma}=J^{-1}\mathbf{FSF}^{\mathrm{T}}$ as follows:

$$\boldsymbol{\sigma}=\boldsymbol{\sigma}^{*}-p\mathbf{I} \text{ with } \boldsymbol{\sigma}^{*}=2\left(W_1\mathbf{b}+\sum_{i=1}^{4}W_{i4}\mathbf{F}\mathbf{M}_i\mathbf{F}^{\mathrm{T}}\right), \tag{7}$$

in which $\mathbf{b}=\mathbf{F}\cdot\mathbf{F}^{\mathrm{T}}$ is the left Cauchy-Green tensor.

2.3 Stress calculation

Considering an arterial wall with internal blood pressure P_{i} in Fig. 1(c), the boundary conditions are

$\sigma_{rr}\left(r_{\mathrm{i}}\right)=-P_{\mathrm{i}}$, and $\sigma_{rr}\left(r_{\mathrm{o}}\right)=0$. (8)

Due to the symmetry of the wall geometry and the boundary conditions, the equilibrium equation $\operatorname{div}\boldsymbol{\sigma}=0$ reduces to

$$\frac{\mathrm{d}\sigma_{rr}}{\mathrm{d}r}+\frac{1}{r}\left(\sigma_{rr}-\sigma_{\theta\theta}\right)=0. \tag{9}$$

Using Eqs. (7) and (8), the integration of Eq. (9) from r_{i} to r_{o} yields

$$P_{\mathrm{i}}=\int_{r_{\mathrm{i}}}^{r_{\mathrm{o}}}\frac{1}{r}\left(\sigma_{\theta\theta}^{*}\left(r\right)-\sigma_{rr}^{*}\left(r\right)\right)dr. \tag{10}$$

Noting that R_{i}, R_{o}, Φ_0, P_{i}, and λ_{z} are the input data, we can obtain r_{i} and r_{o} by numerically solving Eqs. (5) and (10). Then, the Lagrange multiplier $p\left(r\right)$ can be obtained by integrating Eq. (9) from r_{i} to r, that is

$$p\left(r\right)=\sigma_{rr}^{*}\left(r\right)+P_{\mathrm{i}}-\int_{r_{\mathrm{i}}}^{r}\frac{1}{r}\left(\sigma_{\theta\theta}^{*}\left(r\right)-\sigma_{rr}^{*}\left(r\right)\right)dr,\quad r_{\mathrm{i}}\le r\le r_{\mathrm{o}}. \tag{11}$$

By substituting Eq. (11) into Eq. (7), the stress distributions in the arterial wall are then determined.

According to reference Gosling et al. [Gosling and Budge (2003)], the incremental elastic modulus $E_{\mathrm{inc}}=\bar{r}^{2}\,\Delta P_{\mathrm{i}}/\left(h\Delta r\right)\big|_{\Delta P_{\mathrm{i}}\to 0}$ is used to characterize the circumferential stiffness of the FPA wall, in which Δr is the radial deformation of the arterial wall induced by a small pressure change ΔP_{i}, $\bar{r}=\left(r_{\mathrm{i}}+r_{\mathrm{o}}\right)/2$ is the mean radius of the arterial wall, and $h=r_{\mathrm{o}}-r_{\mathrm{i}}$ is the wall thickness.

Because the numerical simulations of the systemic circulation suggest no significant variation of blood pressure along the aorta [Boileau, Nithiarasu, Blanco et al. (2015)], the systolic blood pressures of human common carotid artery are adopted as the internal pressures P_{i} in this study, which contain five stages: 15.8 kPa (baseline), 18.0 kPa (load 1), 20.7 kPa (load 2), 23.2 kPa (load 3), and 25.3 kPa (load 4) as categorized in reference [Hellstrom, Fischer-Colbrie, Wahlgren et al. (1996)].

3 Results

3.1 Stress and strain variations

Fig. 2 illustrates the circumferential stresses in the FPA walls of six age groups from 11 to 70 years old. The variations of the stress distributions during aging process are obvious.

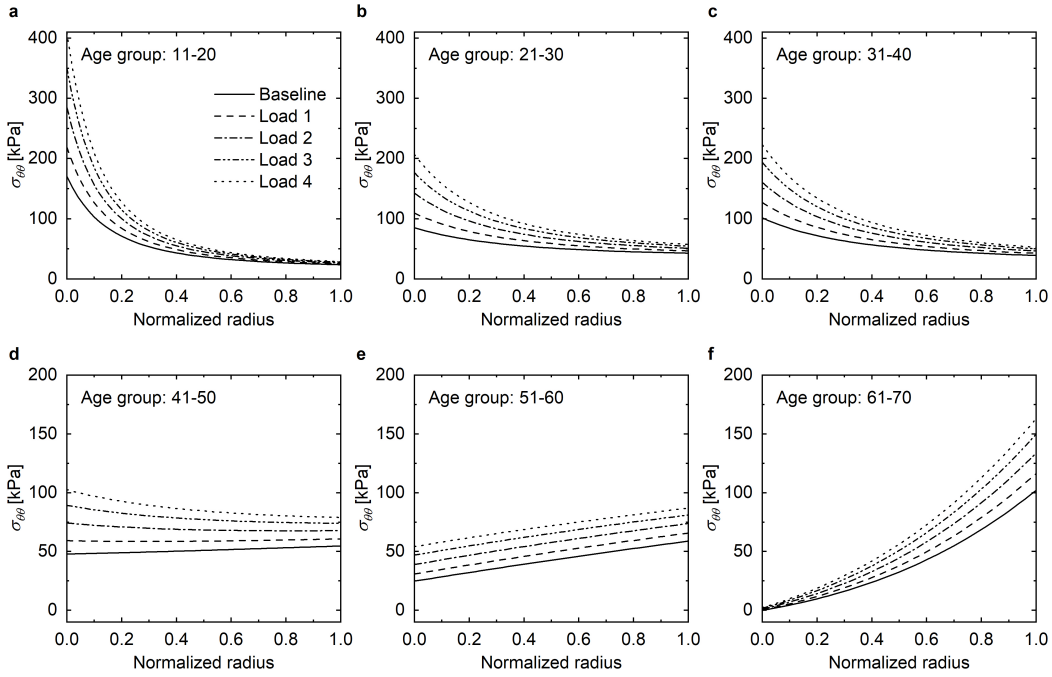

Figure 2: Distributions of circumferential stresses $\sigma_{\theta\theta}$ through FPA walls for different age groups. The normalized radius is $\left(r-r_{\mathrm{i}}\right)/\left(r_{\mathrm{o}}-r_{\mathrm{i}}\right)$, indicating the radial location from the inner wall to outer wall. The internal pressures: baseline=15.8 kPa, load 1=18.0 kPa, load 2=20.7 kPa, load 3=23.2 kPa, and load 4=25.3 kPa

The FPAs younger than 40 years old exhibit an apparent stress decrease along the radial direction (Figs. 2(a), 2(b), 2(c)). For the age group of 11-20 years old, the stress at the inner wall exceeds 400 kPa at the maximum internal pressure of load 4, which is approximately 2.0 times the maximum for the FPAs aged from 21 years to 40 years old. The stresses in the middle-aged FPAs of 41-50 and 51-60 age groups remain constant across the wall thickness (Figs. 2(d), 2(e)). For the 61-70 age group, a stress increase is observed along the radial direction (Fig. 2(f)). The stress at the outer wall increases by 59.7%, up to 162.9 kPa with the internal pressure reaching the maximum, while the stress remains to be zero near the inner wall.

The circumferential stress, strain, and their gradients in the FPA intima, media, and adventitia are plotted along the mean age as shown in Fig. 3. The intima exhibits the most obvious decrease in stress and strain during the aging process, and the maximum decreasing ratios occurs at the age between 16.7 years old and 25.0 years old, as -10.3 kPa per year (Fig. 3(a)) and -0.017 per year (Fig. 3(b)), respectively. The stress in adventitia increases with age by more than 330% during the FPA aging, and it exhibits the largest increase ratio of 5.1 kPa per year after 56.1 years old.

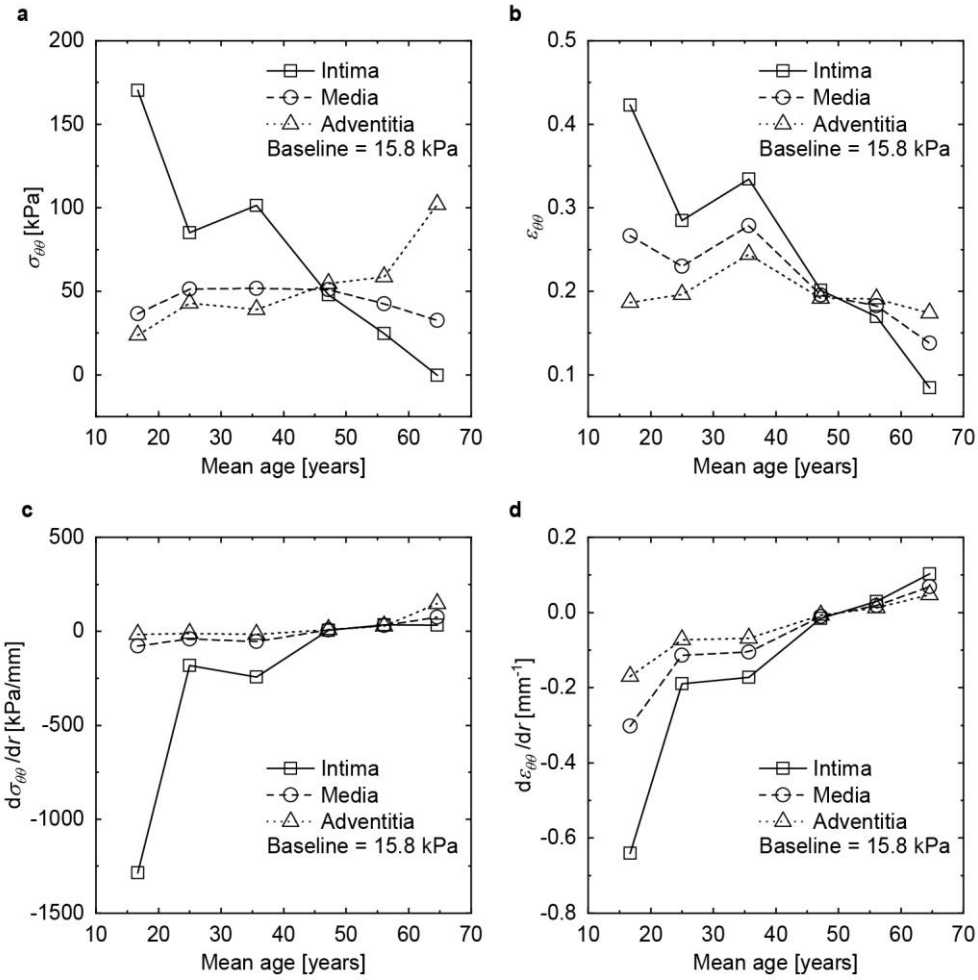

Figure 3: Variations of the stress $\sigma_{\theta\theta}$ (**a**), strain $\varepsilon_{\theta\theta}$ (**b**), stress gradient $\mathrm{d}\sigma_{\theta\theta}/\mathrm{d}r$ (**c**), and strain gradient $\mathrm{d}\varepsilon_{\theta\theta}/\mathrm{d}r$ (**d**) with advancing age at the inner wall (Intima), middle layer (Media), and outer wall (Adventitia) of the FPAs, which characterize the stress variations experienced by endothelial cells (ECs), vascular smooth muscle cells (VSMCs), and fibroblasts in the vessel walls, respectively. The internal pressure is at baseline=15.8 kPa

The stress and strain in intima increase with the age from 25.0 years old to 35.7 years old (Figs. 3(a), 3(b)), however, the gradients maintain a plateau stage (Figs. 3(c), 3(d)). After the age of 35.7 years old, the stress and strain in each FPA layer (intima, media, and adventitia) vary monotonically with age, which suggests that, changes in the mechanical environments with age become irreversible. The magnitudes in the stress and strain gradients gradually decrease with age, and the stress and strain points coincide with each other for the intima, media, and adventitia at around 47.2 years of age, suggesting a uniform distribution. After the age of 50.0 years, the distribution is reversed, namely, low

stress and strain occurring in intima, and high stress and strain in adventitia. In more senior FPAs, the reversed distribution becomes pronounced.

3.2 Wall stiffness

As illustrated in Fig. 4, the FPAs younger than 30 years old exhibit a relative low wall stiffness, however, a sudden increase in wall stiffness is observed from 25.0 years old to 35.7 years old. After 30 years of age, the wall stiffness fluctuates with age to a certain extent.

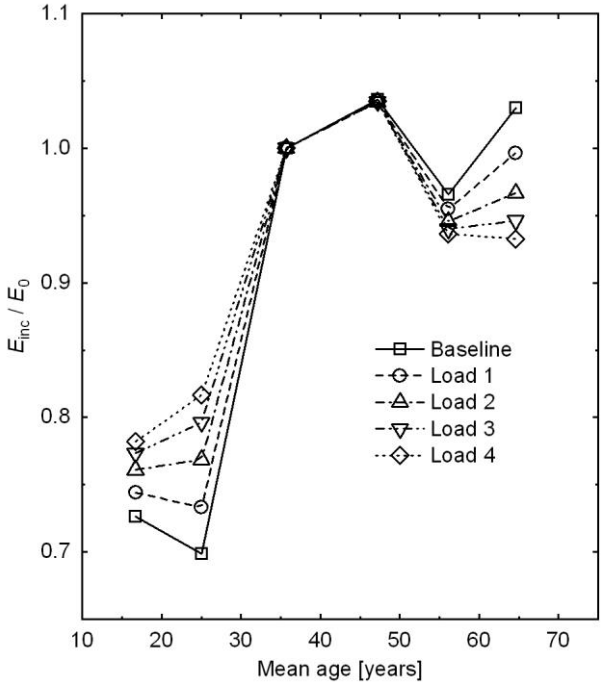

Figure 4: Variations of E_{inc}/E_0 with mean age, where E_{inc} is the FPA wall stiffness, and E_0 is the reference value characterized by the wall stiffness of the FPA at 35.7 years old. E_0=974 kPa, 1210 kPa, 1516 kPa, 1815 kPa, and 2075 kPa at baseline, load 1, load 2, load 3, and load 4, respectively

4 Discussion

Arterial aging is one of the major risk factors causing cardiovascular diseases [Najjar, Scuteri and Lakatta (2005); Lakatta (2002)]. Based on the measured geometries, loading conditions, and material properties during the FPA aging [Tarumi, Ayaz Khan, Liu et al. (2014)], we evaluated the age-related differences in the mechanical niches for vascular cells.

4.1 Mechanobiological indicators for different age groups

4.1.1 The adolescent and young

High strains were observed in the FPAs younger than 40 years old (Fig. 3(b)), which suggested that, the FPA wall is sufficiently compliant to allow large elastic expansion, and the elastin seems to play a dominant role in bearing the tension forces during the wall inflation. However, high blood pressures enhanced the stress concentration near the intima region (Figs. 2(a), 2(b), 2(c)). In terms of cellular mechanotransduction, high stress stimuli are closely associated with endothelial cell (EC) dysfunction and vascular smooth muscle cell (VSMC) death [Cattaruzza, Dimigen, Ehrenreich et al. (2000); Xiong, Hu and Han (2013)]. Therefore, the FPA inflammation and remodeling for adolescent and young subjects are more likely to be initiated by intima damage under hypertensive conditions or acute endurance exercises.

4.1.2 The middle age

The stress in the middle-aged FPA wall exhibited an approximately uniform and linear distribution (Figs. 2(d), 2(e)). It varied slightly with the blood pressure increase, and no stress concentration was observed even under higher blood pressures. This suggested that the FPA wall probably has remodeled itself during the transition from young to middle age, so that it is capable of resisting severe fluctuation of blood pressure, and maintaining a mechanical homeostasis around the vascular cells [Humphrey (2008)].

4.1.3 The elderly

Our results showed that, the stress in the FPA wall tends to decrease with age in intima, but increase in adventitia, contributing to an inverted stress distribution in the FPAs of 61-70 age group (Fig. 2(f)). Recent reviews have demonstrated that the adventitia is mechanosensitive to mechanical stress or injury, and plays a central role in regulating vascular wall function [Stenmark, Yeager, El Kasmi et al. (2013)]. Therefore, high stress observed in older FPA adventitia may induce various vascular diseases by activating the pathological responses of resident cells from the outside in [Psaltis and Simari (2015)].

4.2 Variations of wall stiffness

The wall stiffness of the FPA exhibited a substantial transition from 25.0 years to 35.7 years old (Fig. 4), and subsequently fluctuated with age, which indicated that the 30-year-old may be a critical age. Our results agree with the previous experimental results that muscular arteries older than 30 years of age exhibit no significant difference in wall stiffness [Hayashi, Sugawara, Komine et al. (2005); Bortolotto, Hanon, Franconi et al. (1999)]. We may speculate that the wall stiffness of the FPA is more likely to be affected by vascular developing in the young group rather than aging in the middle-aged and old groups. Therefore, in addition to wall stiffness, more mechanical factors should be considered for evaluating the progress of FPA aging.

4.3 Aging profile of the FPA

In this study, we explored the strain value in FPA intima as a novel aging index for two reasons: 1) it exhibited the most significant variation during the entire life span; 2) its variation was approximately in synchronization with the variation of the mechanical environments in the FPA wall. By fitting the strain of the intima (Fig. 3(b)) with B-Spline curve, we obtained an aging profile as illustrated in Fig. 5, in which the life span was divided obviously.

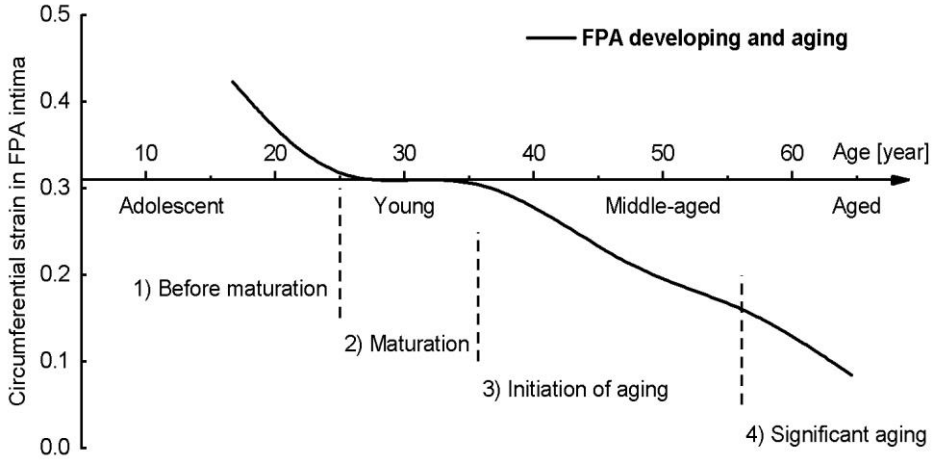

Figure 5: FPA developing and aging during the entire life span, in which four stages are illustrated: 1) before maturation, 2) maturation, 3) initiation of aging, and 4) significant aging

From adolescent to young subjects, the intima exhibited the most significant decreases in stress and strain (Figs. 3(a), 3(b)), which suggested that vascular tissue growth before maturation probably alters the stress responses of the FPA wall.

At around the age of 30 years, the FPA wall suspended the stress and strain decrease in intima, and presented a short-term gradient plateau across the wall thickness (Figs. 3(c), 3(d)). It seems that the FPA matures at this age and it is capable to maintain a stable state in mechanical property. The monotonic change in stress and strain after 35.7 years of age (Figs. 3(a), 3(b) probably implied the irreversible wall remodeling due to the initiation of aging.

For the FPAs older than 56.1 years of age, the stress and strain distributions were quite different from those of adolescent and young FPAs (Figs. 3(a), 3(b)), which indicated an entirely different mechanical environment for the resident cells. The adventitia was like a "jacket", restricting the intima deformation and bearing most of the stress and strain.

4.4 Limitations

In this study, we focused on the age-related variations of the mechanical environments in the FPA wall. The effects of hypertension, diabetes, and smoking were not investigated, while they may also affect the stress responses of arterial wall. Although the arterial wall

has been demonstrated to be heterogeneous in many histological studies, the FPA wall was simplified as a homogeneous single-layer tube due to the lack of layer-specific mechanical properties. The elastic modulus of a vessel wall usually varies along its radial direction, but in this study the averaged elastic modulus was used to quantify the wall stiffness. In addition, the effects of surrounding tissues on the mechanical behaviors of FPA wall were ignored.

5 Conclusions

In this study, we evaluated the aging effects on the mechanical environments in the FPAs aged from adolescent to aged subjects. It was found that high stress region varies with age from the intima for young subjects to the adventitia for old subjects. Uniform stress distribution observed in the middle-aged FPA suggested its remarkable ability in maintaining a mechanical homeostasis during the blood pressure increase. Our results demonstrated that variations of stress and strain rather than that of wall stiffness can be used to evaluate the progress of FPA aging. We hope that the present work could build a credible age-specific mechanical reference for vascular mechanobiological studies, and help elucidate the interaction of cellular mechanotransduction in vascular diseases with human aging process.

Acknowledgement: This work was supported by the National Natural Science Foundation of China (Grants 11872040, 11232010).

References

Boileau, E.; Nithiarasu, P.; Blanco, P. J.; Müller, L. O.; Fossan, F. E. et al. (2015): A benchmark study of numerical schemes for one-dimensional arterial blood flow modelling. *International Journal for Numerical Methods in Biomedical Engineering*, vol. 31, no. 10, pp. 1-33.

Bortolotto, L. A.; Hanon, O.; Franconi, G.; Boutouyrie, P.; Legrain, S. et al. (1999): The aging process modifies the distensibility of elastic but not muscular arteries. *Hypertension*, vol. 34, pp. 889-892.

Cattaruzza, M.; Dimigen, C.; Ehrenreich, H.; Hecker, M. (2000): Stretch-induced endothelin B receptor-mediated apoptosis in vascular smooth muscle cells. *FASEB Journal: Official Publication of the Federation of American Societies for Experimental Biology*, vol. 14, no. 7, pp. 991-998.

Chuong, C. J.; Fung, Y. C. (1983): Three-dimensional stress distribution in arteries. *Journal of Biomechanical Engineering*, vol. 105, no. 3, pp. 268-274.

Desyatova, A.; MacTaggart, J.; Kamenskiy, A. (2017): Constitutive modeling of human femoropopliteal artery biaxial stiffening due to aging and diabetes. *Acta Biomaterialia*, vol. 64, pp. 50-58.

Desyatova, A.; MacTaggart, J.; Romarowski, R.; Poulson, W.; Conti, M. et al. (2018): Effect of aging on mechanical stresses, deformations, and hemodynamics in human femoropopliteal artery due to limb flexion. *Biomechanics and Modeling in Mechanobiology*, vol. 17, no. 1, pp. 181-189.

Fung, Y. C. (1991): What are the residual stresses doing in our blood vessels? *Annals of Biomedical Engineering*, vol. 19, no. 3, pp. 237-249.

Gosling, R. G.; Budge, M. M. (2003): Terminology for describing the elastic behavior of arteries. *Hypertension*, vol. 41, no. 6, pp. 1180-1182.

Han, H. C.; Fung, Y. C. (1996): Direct measurement of transverse residual strains in aorta. *The American Journal of Physiology*, vol. 270, pp. 750-759.

Hayashi, K.; Sugawara, J.; Komine, H.; Maeda, S.; Yokoi, T. (2005): Effects of aerobic exercise training on the stiffness of central and peripheral arteries in middle-aged sedentary men. *Japanese Journal of Physiology*, vol. 55, no. 4, pp. 235-239.

Hellstrom, G.; Fischer-Colbrie, W.; Wahlgren, N. G.; Jogestrand, T. (1996): Carotid artery blood flow and middle cerebral artery blood flow velocity during physical exercise. *Journal of Applied Physiology*, vol. 81, no. 1, pp. 413-418.

Holzapfel, G. A.; Gasser, T. C.; Ogden, R. W. (2000): A new constitutive framework for arterial wall mechanics and a comparative study of material models. *Journal of Elasticity*, vol. 61, no. 1-3, pp. 1-48.

Humphrey, J. D. (2008): Vascular adaptation and mechanical homeostasis at tissue, cellular, and sub-cellular levels. *Cell Biochemistry and Biophysics*, vol. 50, no. 2, pp. 53-78.

Kamenskiy, A, V.; Pipinos, I. I.; Dzenis, Y. A.; Phillips, N. Y.; Desyatova, A. S. et al. (2015): Effects of age on the physiological and mechanical characteristics of human femoropopliteal arteries. *Acta Biomaterialia*, vol. 11, no. 1, pp. 304-313.

Kamenskiy, A.; Seas, A.; Deegan, P.; Poulson, W.; Anttila, E. et al. (2017): Constitutive description of human femoropopliteal artery aging. *Biomechanics and Modeling in Mechanobiology*, vol. 16, no. 2, pp. 681-692.

Kumar, A.; Placone, J. K.; Engler, A. J. (2017): Understanding the extracellular forces that determine cell fate and maintenance. *Development*, vol. 144, no. 23, pp. 4261-4270.

Lakatta, E. G. (2002): Age-associated cardiovascular changes in health: impact on cardiovascular disease in older persons. *Heart Failure Reviews*, vol. 7, no. 1, pp. 29-49.

McEniery, C. M.; Yasmin, Hall I. R.; Qasem, A.; Wilkinson, I. B. et al. (2005): Normal vascular aging: Differential effects on wave reflection and aortic pulse wave velocity-The Anglo-Cardiff Collaborative Trial (ACCT). *Journal of the American College of Cardiology*, vol. 46, no. 9, pp. 1753-1760.

Najjar, S. S.; Scuteri, A.; Lakatta, E. G. (2005): Arterial aging: is it an immutable cardiovascular risk factor? *Hypertension*, vol. 46, no. 3, pp. 454-462.

Psaltis, P. J.; Simari, R. D. (2015): Vascular wall progenitor cells in health and disease. *Circulation Research*, vol. 116, no. 8, pp. 1392-1412.

Sears, C.; Kaunas, R. (2016): The many ways adherent cells respond to applied stretch. *Journal of Biomechanics*, vol. 49, no. 8, pp. 1347-1354.

Stenmark, K. R.; Yeager, M. E.; El Kasmi, K. C.; Nozik-Grayck, E.; Gerasimovskaya, E. V. et al. (2013): The adventitia: Essential regulator of vascular wall structure and function. *Annual Review of Physiology*, vol. 75, no. 1, pp. 23-47.

Tarumi, T.; Ayaz Khan, M.; Liu, J.; Tseng, B. M.; Parker, R. et al. (2014): Cerebral hemodynamics in normal aging: Central artery stiffness, wave reflection, and pressure pulsatility. *Journal of Cerebral Blood Flow and Metabolism*, vol. 34, no. 6, pp. 971-978.

Wheeler, J. B.; Mukherjee, R.; Stroud, R. E.; Jones, J. A.; Ikonomidis, J. S. (2015): Relation of murine thoracic aortic structural and cellular changes with aging to passive and active mechanical properties. *Journal of the American Heart Association*, vol. 4, no. 3, e001744.

Xiong, Y.; Hu, Z.; Han, X.; Jiang, B.; Zhang, R. et al. (2013): Hypertensive stretch regulates endothelial exocytosis of Weibel-Palade bodies through VEGF receptor 2 signaling pathways. *Cell Research*, vol. 23, no. 6, pp. 820-834.